Multi-omics study of keystone species in the cystic fibrosis lung microbiome

Cynthia Silveira (cynthiabsilveira@gmail.com)
University of Miami https://orcid.org/0000-0002-9533-5588
Ana Georgina Cobian-Guemes
San Diego State University
Carla Uranga
J Craig Venter Institute
Jonathon Baker
J Craig Venter Institute
Anna Edlund
J Craig Venter Institute
Forest Rohwer
San Diego State University
Douglas Conrad
University of California San Diego

Research

Keywords: clindamycin, anaerobes, fermentation, mucus plugs, WinCF, metagenomics, metabolomics, transcriptomics

Posted Date: March 25th, 2020

DOI: https://doi.org/10.21203/rs.3.rs-18792/v1

Multi-omics study of keystone species in the cystic fibrosis lung microbiome

Cynthia B. Silveira[1,2,3], Ana G. Cobian-Guemes[2,3], Carla Uranga[4], Jonathon Baker[4], Anna Edlund[4], Forest Rohwer[2,3] and Douglas Conrad[5]

[1] Department of Biology, University of Miami, 1303 Memorial Dr., FL 33146, USA.

[2] Department of Biology, San Diego State University, 5500 Campanile Dr., CA 92182, USA.

[3] Viral Information Institute, San Diego State University, 5500 Campanile Dr., CA 92182, USA.

[4] J. Craig Venter Institute, Genomic Medicine Group, La Jolla, CA, 92037, USA.

[5] Department of Medicine, Division of Pulmonary, Critical Care and Sleep Medicine, University of California San Diego, La Jolla, California, USA.

cynthiasilveira@miami.edu, ana.naiboc@gmail.com, curanga@jcvi.org, jobaker@jcvi.org, aedlund@jcvi.org, frohwer@gmail.com, dconrad@ucsd.edu

Correspondence to: cynthiasilveira@miami.edu

Kew words: clindamycin, anaerobes, fermentation, mucus plugs, WinCF, metagenomics, metabolomics, transcriptomics

Abstract

Background: Ecological networking and *in vitro* studies have predicted that anaerobic, mucus-degrading bacteria are keystone species in cystic fibrosis (CF) microbiomes by sustaining the growth of canonical CF pathogens. Here, a multi-omics approach was deployed to test this hypothesis *in vivo* and in real time during a transition in antibiotic therapy of a CF patient with a hypervariable lung function phenotype.

Results: Quantitative meta-omics and community culturing demonstrated that the use of a non-traditional clindamycin therapy targeting gram-positives and gram-negative anaerobes re-structured the entire CF microbial community. During rapid lung function loss, when the patient was off antibiotics, the microbial community was dominated by anaerobic mucus-degrading *Streptococcus* sp., *Veilonella* sp., and *Prevotella* sp. that produced fermentation gas and led to the accumulation of fermentation products in sputum. The rise of anaerobes was followed within 6 days by an increase in *Pseudomonas aeruginosa* transcripts encoding the acquisition of fermentation products from anaerobes and the production of virulence factors. The initiation of clindamycin treatment reduced the fermentation and the abundance of anaerobes. Clindamycin also lowered the abundance and transcription of *P. aeruginosa,* which is resistant to this antibiotic. The treatment stabilized the patient's lung function and improved respiratory health for two months, lengthening by a factor of four the between-hospitalization time for this patient.

Conclusions: The results presented here show that killing anaerobes, the weakest link in the community in terms of antibiotic resistance, effectively limited the growth of classic CF pathogen by disrupting community cross-feeding. The role that anaerobic, mucus-degrading bacteria played in structuring the CF microbiome corroborates *in vivo* their position as keystone bacteria, with high impact on community function despite lower relative abundances.

Introduction

Keystone species are members of a community that have a disproportionately high importance in ecosystem stability despite being less abundant than other community members [1]. In the ecology of macro-organisms, these species commonly include top predators and first-level consumers, which control ecosystem energy flow and, therefore, structure trophic relationships [2, 3]. In the human microbiome, this ecological concept gave rise to the keystone-pathogen hypothesis, which posits that "certain low-abundance microbial pathogens can orchestrate inflammatory disease by remodeling a normally benign microbiota into a dysbiotic one" [4]. However, microbial ecology studies identify keystone species mainly based on their central position in network analyses [5, 6]. One caveat of this approach is that metabolic networks are often built based on co-occurrence relationships in microbiomes (metagenomics) or their activities (transcriptomics) [7, 8]. Identifying true keystone species require manipulative studies of the microbiome [9, 10]. Clinical treatment of polymicrobial diseases using narrow spectrum antibiotics mimics this experimental approach and offers an invaluable opportunity to investigate keystone species of the human microbiome *in vivo*.

Cystic fibrosis (CF) patients suffer from chronic polymicrobial infections throughout their lives and are often treated with multiple antibiotics since early age [11]. Altered anion (Cl^- and bicarbonate) transport in the CF respiratory epithelium result in decreased mucociliary clearance and antimicrobial innate defenses, allowing the chronic colonization by a polymicrobial community [12–15]. These communities elicit strong innate immune responses that drive the airway wall remodeling and gas exchange abnormalities, eventually resulting in respiratory failure or a need for lung transplantation in over 80 % of CF patients. The polymicrobial nature

of CF airway infections [11, 16–20] led to Climax-Attack ecological model the of the CF lung microbiome [21]. The Attack community consists of transient members that elicit strong innate immune responses and acute deterioration [22, 23]. In contrast, Climax communities cause chronic infections and include most of the classic CF pathogens, including *P. aeruginosa,* which are inherently resistant to anti-microbial therapy, grow slowly forming biofilms, and generate suboxic environments in mucus plugs [24–26]. Hypoxic metabolisms are common in CF patients with advanced lung disease or during exacerbations, when microbes use alternative electron acceptors (nitrates, sulfates, iron, and fumarate) and fermentation [22, 27, 28], accumulating toxic metabolic products in the lung [29, 30].

Previous network analysis and *in vitro* studies suggested that anaerobic bacteria function as keystone species sustaining the microbial community and disease progression in CF [31, 32]. The mechanistic basis of this hypothesis is the cross-feeding that occurs as mucin-degrading anaerobes release fermentation products that sustain the growth of pathogens such as *P. aeruginosa*, an inefficient mucus-degrading bacterium. Long-term 16S rRNA studies have also shown an association between higher relative abundance of anaerobic bacteria including *Streptococcus sp.* and *Veillonella sp.* with better health when *P. aeruginosa* is absent [33]. Here, the onset of clindamycin treatment specifically targeting gram-positives and gram-negative anaerobes during the clinical care of a CF patient offered an invaluable opportunity to test *in vivo* the hypothesis that anaerobes are keystone species in CF. Quantitative multi-omics combined with a community culture system showed that clindamycin suppressed not only anaerobes but also *P. aeruginosa.* The disturbance of microbial cross-feeding improved the health of this patient by extending the between-hospitalization time by a factor of four.

Results

Clinical data: Patient 146 is part of the highly variable lung function group according to his percent predicted Forced Expiratory Volume in 1 second (ppFEV1) [34]. In the year preceding this study, the patient experienced 10 periods of rapid lung function loss that led to hospitalization and intravenous (IV) antibiotic treatments (Supplementary Figure 1). The ppFEV1 varied between 38 and 67 % during that year (median = 53 ± 5.7 SD). The clinical microbiology tests were positive for *P. aeruginosa*, however the patient could not be stabilized with oral antibiotic treatment after each hospital discharge. With the goal of identifying potential causes for this hypervariable phenotype, a CF Rapid Response (CFRR) was launched at the time of an exacerbation event in which the patient was admitted to the hospital for intravenous antibiotic treatment [35]. During the Rapid response, metagenomes, transcriptomes and metabolomes, community cultures and direct microbial counts were obtained from expectorated sputum samples and analyzed in real-time (see Methods). At Day 0 (First day of CFRR), the patient displayed acute decline in respiratory health characterized by severe cough, dyspnea and a drop in his ppFEV1 to 44 %, 9 % below his median ppFEV1 (Figure S1). In the 27 days of hospitalization that followed, the patient was treated with colistin, vancomycin, piperacillin-tazobactam, and ceftazidime-avibactam, and the ppFEV1 increased to 59 %, leading to the patient's discharge. This hospitalization period will be referred to as period A in this study. During the following 8 days, named period B, he was off antibiotics. On day 33, six days after hospital discharge, his ppFEV1 rapidly decreased to 50% and the patient complained of intense cough and shortness of breath. Oral clindamycin treatment was initiated, and improved overall

112 symptoms including cough and shortness of breath and maintained ppFEV1 at 49 %. This is
113 referred to as period C. The clinical microbiology tests were positive for *P. aeruginosa* before
114 CFRR, and a targeted search detected *Rothia mucilaginosa* in the clinical laboratory after it was
115 detected in the meta-omics data through CFRR (the dates of clinical microbiology tests are
116 shown in Figure S1). The patient was not under CFTR modulator treatment.
117
118 *Microbial community structure:* To investigate the community structure transitions across
119 changes in antibiotic regime and health status in Periods A, B and C, data from taxon-specific
120 microbial abundances, transcriptional activities, *in vitro* community culture (WinCF in Methods)
121 and total microbial abundances were analyzed by unsupervised random forest, a statistical
122 learning algorithm for identification of sample clusters and variables of importance. The random
123 forest identified three clusters of samples characterized by the patient's health status (Figure 1a
124 shows a 2D projection of the samples from a non-metric multidimensional scaling (NMDS)
125 analysis and clusters identified by the random forest are indicated by the dotted ellipses). The
126 first cluster includes samples from periods of lowest ppFEV1 and worst symptoms (cough and
127 shortness of breath) and coincides with highest WinCF fermentation and highest *P. aeruginosa*
128 abundance and transcriptional activity (cluster in the center of the NMDS plot in Figure 1a). The
129 antibiotic treatment in period A drove the community to a state of low microbial load and
130 correlated with the abundance and transcriptional activity of *Rothia mucilaginosa* (cluster on
131 right side of Figure 1a). As health deteriorated in period B, the abundance of *Streptococcus*,
132 *Staphylococcus* and *Veillonella* increased (also identified as cluster 2 in Figure 1a). This state
133 was followed by a return to low lung function with high fermentation, and high *Pseudomonas*
134 abundance and transcriptional activity (cluster 1 in the center Figure 1a). The onset of

clindamycin treatment in period C drove the community to a third state, characterized by *Neisseria* sp. and *Haemophilus* sp. abundance and transcriptional activity, with low total microbial load and fermentation (cluster on the left side of Figure 1a). The random forest indicated that the abundance of *Streptococcus* was the most important variable differentiating the three clusters, followed by the abundance of *Pseudomonas* and *Streptococcus* transcriptional ascitivies. A second random forest analysis supervised by the antibiotic regimes (periods A, B and C) showed an out of bag error rate estimate of 11.1 %, in which *Streptococcus* abundance was the variable with highest importance differentiating the periods, followed by *Rothia, Staphylococcus, and Haemophilus* transcriptional activities (Figure 1b, p-values in the permutational random forest test were 0.002, 0.009, 0.02, and 0.04, respectively).

The results of this multivariate statistical analysis led to the hypothesis that fermentation products of mucus-degrading facultative anaerobes facilitated the rise of Pseudomonas aeruginosa, a classical CF pathogen, through cross-feeding (Figure 1c). This mechanism of interaction has been previously shown *in vitro* [32] and generated the following specific predictions that could be tested with our dataset: 1- Facultative anaerobes, including *Streptococcus* and *Rothia*, efficiently degrade mucus producing free-amino acids and short-chain fatty acids (SCFA, i.e., propionate, acetate, butyrate, and butanediol). 2- The free amino acids and SCFAs open a niche for the growth of *Pseudomonas*, which degrades mucins poorly. *Pseudomonas* grows forming an anaerobic biofilm and produces phenazines. 3- The anoxic biofilm created by *Pseudomonas* facilitates the growth of strict anaerobes, including *Veillonella* and *Prevotella*. The whole microbial community grows, with *Pseudomonas* benefitting from the metabolic products from anaerobes. 4- The onset of clindamycin treatment suppresses mucus-

158 degrading anaerobes, destabilizing the community by the removal of the main nutritional source
159 for *Pseudomonas*, and decreasing total microbial abundances. How the meta-omics dataset met
160 the predictions of this working model is explored in detail in the following sections.
161
162 *Bacterial abundances:* Direct epifluorescence counts of bacterial cells were combined with
163 sputum metagenomes to quantify total bacterial load and taxon-specific abundances in cells per
164 ml. The bacterial load in the sputum sample collected at Day 1 was 6.71×10^8 cells per ml, and
165 the community was dominated by *Rothia mucilaginosa* (78 % of the community, Figure 2a).
166 After 2 weeks of intravenous antibiotic in Period A, the bacterial load decreased to 2.9×10^7,
167 with most members of the community decreasing their absolute abundance, except for
168 *Staphylococcus aureus* and *Veillonella dispar*. In Period B, when the patient was off antibiotics,
169 the microbial abundance increased to 2.6×10^8. At this point, *S. aureus* and *Streptococcus*
170 *sanguinis* were the most abundant bacteria, followed by *R. mucilaginosa* and *P. aeruginosa*. The
171 clindamycin treatment (Period C) decreased microbial load to 2.4×10^7, and the community
172 became dominated by *Haemophilus* sp. and *Neisseria* sp. Both *Haemophilus* sp. and *Neisseria*
173 sp. decreased in abundance to less than 0.001 % of the community after 2 months.
174
175 *Bacterial transcriptional activity:* Transcriptomes were mapped to the draft genome sequences
176 of *Rothia mucilaginosa*, *Streptococcus sanguinis*, *Staphylococcus aureus*, *Veillonela dispar,* and
177 *Pseudomonas aeruginosa* obtained from colonies isolated from the patient's sputum. The most
178 active community members were *R. mucilaginosa*, *S. sanguinis*, *V. dispar*, and *P. aeruginosa,*
179 respectively (Figure 2b). *S. aureus* was not among the most transcriptionally active, despite
180 representing up to 54 % of the community three days post hospital discharge, according to

metagenomic data. Antibiotic treatments changed the transcriptional activity: during intravenous colistin, *R. mucilaginosa* was the most active member, followed by *S. sanguinis* and *V. dispar*. Upon release from antibiotics, *V. dispar* transcripts increased, followed by *S. sanguinis* and *R. mucilaginosa*. After six days off antibiotics, *P. aeruginosa* became the most active member of the community, followed by *S. sanguinis*. Oral clindamycin treatment decreased transcript abundance not only in the target species *S. sanguinis*, but also in *V. dispar*, *R. mucilaginosa* and *P. aeruginosa*.

Fermentation: On Day 1, the WinCF community culture system produced the fermentation gas that occupied 19 % of the WinCF tube (Figure 3a). Simultaneously, the pH decreased in the tube from 7.4 to below 5 starting at 0.33 mm (Figure 3b). The depth of tube where the pH changes corresponds to the transition from the oxic to anoxic environment and is analogous to the oxygen penetrance in the mucus plugs in the lung [29]. The amount of fermentation gas decreased to non-detectable after 2 weeks of antibiotic treatment in period A (Figure 3a), and the depth of pH change in the tubes increased (Figure 3b). After the hospital discharge, gas production increased to 42 % (Figure 3a). This period corresponded to a decrease in pH change depth to 0 mm (Figure 3b), loss of lung function, and overall deterioration of his health. The patient initiated clindamycin treatment 9 days after the hospital discharge, causing a sustained decrease in the fermentation levels, down to to 4 % after the first day of clindamycin and remaining below 3 % for 60 days.

Metabolomes: The GC-MS metabolomic profiles showed that during the period the patient was off antibiotics, there was an increase in the abundance of fermentation products (Figure 3c).

Lactic acid, acetic acid and propanoic acid peaked 6 to 8 days after the patient stopped intravenous colistin treatment and coincided with the increase in fermentation gas and deterioration of heath (Figure 3a). There was also an increase in the abundance of free amino acids and butaneidioic acid, a product of the metabolism of 1,4-butanediol.

Transcription of fermentation-related genes: The acetoin metabolism genes responsible for the synthesis of the 2,3-butenediol and butanedione, a key metabolite in the cross-feeding between *Streptococcus* and *Pseudomonas,* were transcriptionally active in patient CF146 [30]. The genes encoding acetoin biosynthesis acetolactate synthase (*budB*), acetolactate decarboxylase (*budA*), and butanediol dehydrogenase (*budC*) were expressed by *Streptococcus* sp. and *Staphylococcus* sp. at higher levels in periods of lung function loss (Figure 4a). *Rothia* also expressed *budB* early in the sampling period, and *Haemophilus* and *Neisseria* expressed these genes after the onset of clindamycin treatment. *Pseudomonas* aeruginosa was the main taxon expressing the genes *acoA* and *acoB*, whose products catabolize acetoin for utilization in central metabolism (Figure 4b). The expression of *aco* genes was followed by the expression of phenazine by *P. aeruginosa* (Figure 4b), a virulence factor that acts as alternative electron acceptor allowing *P. aeruginosa* thrive in anoxic regions of biofilms and mucus plugs.

Discussion

Microbial colonization of the lungs in CF patients represents a case of complex microbial dysbiosis driving disease progression, often without the identification of an individual causative pathogen [25]. Metabolic networks have predicted that *Streptoccoccus*, *Prevotella* and

Veillonella are the genera with the highest *keystoneness* in CF [31]. These species are efficient mucus-degraders, and their anaerobic metabolism releases short-chain fatty acids that sustain the growth of *P. aeruginosa* [32]. Our community-culture and multi-omics data show that these pathways are active in the lungs of CF146. The growth of *Streptococcus* and *Veillonella* was followed within two days by the growth of *Rothia* and *Pseudomonas* when the patient was off antibiotics (Figures 3 and 4). The production of fermentation gas in the WinCF tubes and the increase in abundance of short-chain fatty acids in the metabolomes demonstrates the activity of fermenting bacteria and the release of metabolic by-products in sputum. Volatile fermentation products such as lactic acid and 2,3-butanediol have been previously detected in CF breath gas [30, 36]. These molecules can induce pyocyanine production, dormancy and biofilm formation in *P. aeruginosa*, stimulating its growth and virulence [37, 38]. 2,3-butanediol has a direct toxic effect on human cells [30]. The combined effects of fermentation products by direct attack to host tissue and by stimulation of pathogen growth were the likely cause of the patient's lung function decline in this study (ppFEV1 dropped from 59 to 50 % six days post hospital discharge).

The drop in lung function with an increase in anaerobic taxa and fermentation during period B (no antibiotics) triggered the initiation of clindamycin treatment, a semisynthetic derivative of lincomycin acting on ribosome translocation that inhibits protein synthesis in facultative gram-positives such as *Staphylococcus* and *Streptococcus*, and anaerobic gram-negatives including *Bacteroides*, *Fusobacterium* and *Prevotella* [39]. Clindamycin reduced the abundance and activity of not only anaerobes, but also that of *P. aeruginosa*, which is resistant to this drug (Figure 2). The decrease in *Pseudomonas* indicates its dependency on *Streptococcus* and

Veillonela byproducts for growth. *Pseudomonas*'s large genome is highly adapted to mucus plugs, encoding alternate oxidative metabolism and virulence factors [40]. Yet, *P. aeruginosa* grows poorly on mucins and depends on cross-feeding by mucus-fermenting anaerobes [32]. *In vitro* antibiotic challenge targeting a mucin-fermenting community containing *Veillonella parvula*, *Fusarium nucleatum*, *Prevotella melaninogenica*, and *Streptococcus parasanguis* in co-cultures with *P. aeruginosa* controled both the fermenters and *P. aeruginosa* [41]. These experiments demonstrated that the whole community minimum inhibitory concentration drops to that of the weakest link – the least resistant species that provides resources to other community members [41]. The dataset presented here provides evidence that this phenomenon occurs *in vivo* and corroborates the role *of Streptococcus* and *Veillonella* as keystone genera in the CF microbiome.

The conclusions presented here are based on an in-depth study of the lung disease progression in one patient. Given the highly personalized nature of the CF microbiome, this pattern should be tested in a larger cohort in the future. Previous studies with larger samples sizes based on 16S rRNA data have shown that low diversity and dominance of a single pathogen are indicative of rapid lung function loss [33]. This pattern is consistent with the concept of keystone species presented here, where microbial community members with low abundance in the microbiome have disproportionality high importance in community function, such as nutritionally sustaining a dominant pathogen. While the multi-omics strategy presented here is still expensive for wide deployment in the CF patient population, the WinCF cultures can be easily performed to indicate fermentation, allowing selection of patients for in-depth studies. Regarding the non-traditional application of clindamycin to treat CF lung infections, its long-term use can facilitate the

development of colitis by *Clostridium difficile* colonization [42]. The suppression of keystone species and metabolisms presented here offers a potential new focus for the the development of novel strategies to manipulate the CF microbiome.

Conclusion

Here we show that a transition in antibiotic treatment of a CF patient re-structures the entire CF microbiome by the suppression of keystone species that nutritionally sustained the growth of a pathogen. Clindamycin therapy targeting anaerobes reduced fermentation and the abundance of both anaerobes and *P. aeruginosa,* which is resistant to this antibiotic. The treatment improved respiratory health for 2 months, lengthening by a factor of four the between-hospitalization time for this patient. These results corroborate in vivo the hypothesis that anaerobes are keystone members of the CF microbiome providing structure and stability to the whole microbial community through cross-feeding.

Methods

Clinical data: Sample collection procedures and access to clinical data were approved by the institutional review boards (IRBs) of the University of California San Diego (UCSD) (HRPP 081510), and San Diego State University (IRB approval number 1711018R). Clinical microbiology and spirometry tests were performed for clinical indications during the normal care of the patient. Spirometry tests were used to calculate the percentage of predicted FEV1 (forced expiratory volume in one second), as previously described [43]. The age*FEV1% predicted

296 product is a derived variable calculated by multiplying the age of the individual at the most
297 recent FEV1 by the best FEV1% during the previous year and is used to assess disease risk [34,
298 44].
299
300 *WinCF community culture:* Winogradsky CF community culture was modified from Quinn *et al*
301 *2015 by* adjusting the pH 7.4 prior to use in WinCF experiments [29, 45–47]. Briefly, sputum
302 samples were collected by expectoration, homogenized, and diluted 10-fold into sterile ASM.
303 The mixture was inoculated into capillary tubes that were plugged at one end and then laid
304 horizontally in a 100% humidity environment at 37 ºC. At the end of incubations, capillary tubes
305 were imaged in the dark on white backlight (Logan 5.5 X 9 inches^2 light box) using a Canon
306 EOS Rebel T3 camera (Canon U.S.S Inc., Melville, NY, USA). All images were taken under
307 identical settings (manual focus, ISO 3,200, Aperture F4.5) and saved in raw and JPEG format.
308 Gas production was quantified as the percentage of capillary tube length occupied by gas. The air
309 penetrance in the capillary was defined as depth of the tube where pH dropped below 5, as
310 indicated by color change in the phenol red/bromocresol purple tubes (pH drops due to
311 fermentation products).
312
313 *Metagenomes:* Total DNA was extracted from sputum samples using an adapted PowerSoil
314 DNA Isolation kit protocol (Qiagen, Germany). The samples were subject to 5 freeze-thaw
315 cycles (5 minutes flash-freeze, 5 minutes at 100 ºC) followed by bead-beating for 45 minutes
316 using the bead tubes from the Power Soil kit. The DNA was eluted in molecular-grade water and
317 metagenome libraries were constructed using a Nextera DNA library preparation kit (Illumina,
318 CA). Libraries were sequenced on an Illumina MiSeq platform. Quality filtering and

dereplication were done using PRINSEQ++ [48] with minimum quality threshold 20, dereplication and entropy threshold 50. Cloning vector sequences were removed using SMALT [49] with 80 % identity against the NCBI UniVec database. Human genome sequences were removed using SMALT with 80 % identity against the human reference genome GRCh38. Microbial taxonomy assignments at the genus level were made from SMALT a with 96 % identity against the NCBI RefSeq database of complete bacterial genomes.

Bacterial isolation and genome sequencing: Fresh sputum sample from the first day of hospitalization in this study (Day 0) were resuspended in saline buffer and plated on BHI agar. Plates were incubated overnight at 37 °C. Colonies with distinct morphologies were picked and re-plated on BHI plates. The five species that represented the most abundant members in the metagenomes (by sequence recruitment at 96% identity) were selected for full genome sequencing: *Rothia mucilaginosa*, *Streptococcus sanguinis*, *Staphylococcus aureus*, *Veillonela dispar* and *Pseudomonas aeruginosa*. Total DNA was extracted and prepared for sequencing using KAPA HyperPlus (KAPA Biosystems, IN). The libraries were sequenced on an Illumina MiSeq platform. Quality filtering, dereplication and cloning vector removal were performed as above. Sequences were assembled using Spades [50].

Metabolomics: Sputum samples (1 ml) were lyophilized before extraction to concentrate all metabolites. Samples were extracted and subjected to fast chemical derivatization reaction using methyl chloroformate [51]. Samples were analyzed by gas chromatography–mass spectrometry (GC-MS). The data was analyzed using Automated Mass Deconvolution and Identification System (AMDIS).

342

343 *Metatranscriptomics:* Total RNA was extracted from raw sputum samples using guanidinium
344 thiocyanate according to manufacter's protocol (TRIzol, Invitrogen, CA). RNA was resuspended
345 in 50 µl of RNAse-free water and DNase treatment was performed by adding 2 µl of TURBO
346 DNase (Thermo Fischer Scientific, CA). First strand RNA was synthesized using Superscript II
347 reverse transcriptase (Invitrogen, CA). Sequencing libraries were prepared using the Ovation
348 Complete Prokaryotic RNA-Seq System (NuGEN Technologies, CA). Libraries were sequenced
349 in an Illumina HiSeq Platform. Quality filtering, dereplication and cloning vector removal were
350 performed as above. The transcripts were mapped to the NCBI RefSeq database of complete
351 bacterial genomes using SMALT at 96 % identity. The number of transcripts mapping to a
352 genome was normalized by genome size using the FRAP to calculate relative number of
353 transcripts mapping to a given taxon within a sample. This relative transcriptional activity was
354 then multiplied by the number of cells per ml of sputum sample to obtain the taxon-specific
355 transcriptional activity per ml of sputum and allow between-sample comparison. This scaling
356 assumes that the total bacterial transcriptional activity per ml of sputum is proportional to the
357 bacterial abundance per ml of sputum. We also mapped the transcripts to the genomes of
358 bacterial isolates obtained from the same patient at 96 % identity using SMALT. The relative
359 transcript abundance was normalized by absolute microbial abundances per ml of sample to
360 allow between-sample comparisons. The transcript recruitment to the isolates genomes was
361 visualized using ANVI'O [52].

362

363 *Multivariate analyses:* The absolute abundance of each genus of bacteria per ml was calculated
364 as the product of the fractional abundance in the metagenome [53] and the total microbial

abundances determined by direct epifluorescence counts. The absolute abundances were combined with taxon-specific transcriptomic activity per ml, WinCF fermentation and total microbial abundances in one dataset (Supplementary Data 1) and analyzed through a non-metric multi-dimensional scaling (NMDS) using Bray-Curtis distances in the vegan package in R. The two first dimensions are visualized in 2D in Figure 1A. Samples were clustered using the proximity matrix from an unsupervised random forest in the R package randomForest using 5000 trees and Ward method for hierarchical clustering. Random forest is a robust non-parametric, statistical learning method for the identification of clusters and variables of importance in complex multi-omics data [54, 55]. The effect of different antibiotic regimes (clindamycin, no antibiotics and the combination of colistin, piperacillin-tazobactam, ceftazidime-avibactam, and vancomycin) on was tested using a supervised permutational random Forest (5000 trees 1000 permutations) where the three antibiotic regimes were used as supervising variable in the package rfPermute.

Declarations

Ethics approval and consent to participate

Sample collection procedures and access to clinical data were approved by the institutional review boards (IRBs) of the University of California San Diego (UCSD) (HRPP 081510) and San Diego State University (IRB approval number 1711018R).

Consent for publication

No identifiable data is included in this manuscript and this study was approved by the institutional review boards of the University of California San Diego (UCSD) (HRPP 081510) and San Diego State University (IRB approval number 1711018R)..

Availability of data and materials

Metagenomic data is available in the NCBI Short Read Archive (SRA) under BioProject ID PRJNA580503. Genome sequences of clinical isolates are provided as contigs and associated annotation files in the Pathosystems Resource Integration Center (PATRIC) server in the public workspace csilveira / CF146. Transcriptomic data are available through the Gene Expression Omnibus (GEO) server in NCBI record GSE139943. Codes used for statistical analysis are provided in github under cbsilveira/CF146 and csv files used as input are provided as Additional Data along with the manuscript.

Competing Interests

The authors declare no competing interests.

Funding

This research was funded by the Cystic Fibrosis Research Inc. (S00022215 to CS and S00023377 to FR) and Spruance Foundation.

Authors' contributions

CBS, FR and DC designed the study; CBS, AGCG, CU, JB and AE performed experiments, analyses; CS wrote the manuscript and all authors contributed with revisions.

Acknowledgements

The authors thank Ryan Hunter, Stephanie Widder and Katrine Whiteson for discussions and criticisms on cross-feeding, keystone species, and metabolomic data that significantly improved this manuscript.

Figures

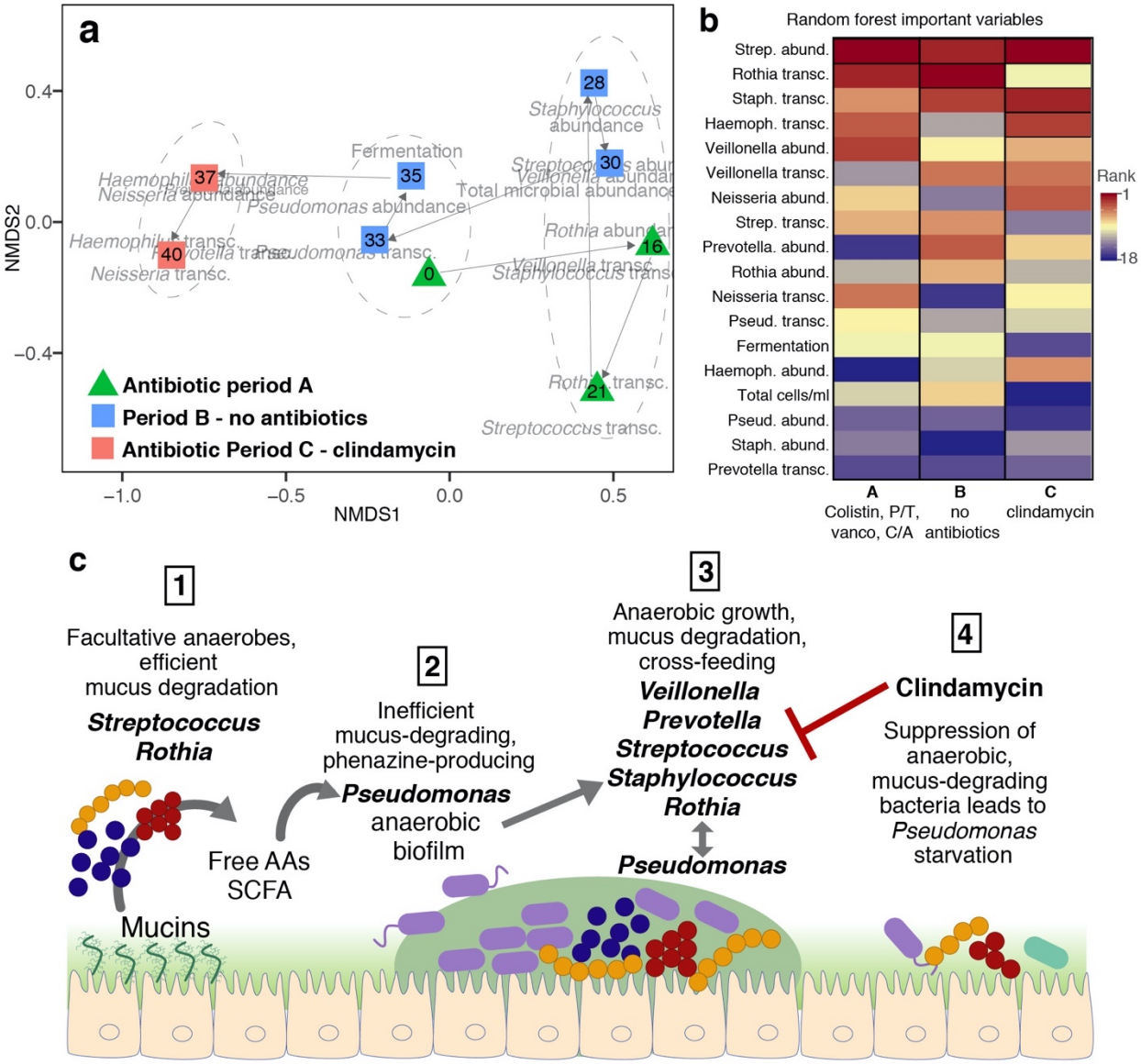

Figure 1. Microbial community succession. a) Non-metric multidimensional scaling (NMDS) of sputum samples over time. The variables used as input for the NMDS were WinCF fermentation, total microbial abundances, genera-specific microbial abundances, and genera-specific transcriptomic activity. Symbols are color-coded by antibiotic treatment periods (green: A - colistin, vancomycin, ceftazidime-avibactam, and piperacillin-tazobactam; blue: B - no

antibiotics; pink: C - clindamycin), and numbers inside the symbols indicate days since hospital admission event when Rapid Response was initiated. The dotted ellipses indicate health status groups supported by an unsupervised random forest analysis followed by clustering using Ward distances (out of bag error = 11.1 %). **b**) Important variables differentiating treatment periods in a classification random forest analysis supervised by treatments. The ranks surrounded by a black box indicate variables with p-values less than 0.05 in the permutational test. **c**) Conceptual model of succession events in patient CF146: 1- The mucosal surfaces are colonized by facultative anaerobes, including *Streptococcus* and *Rothia*, capable of efficient mucus degradation producing free-amino acids and short-chain fatty acids (SCFA, i.e., propionate, acetate, butyrate, and butanediol). 2- The free amino acids and SCFAs open a niche for the growth of *Pseudomonas*, which degrades mucins poorly. Pseudomonas grows forming an anaerobic biofilm, and produces phenazines. 3- The Pseudomonas biofilm facilitates the growth of anaerobes, including obligate anaerobes such as *Veillonella* and *Prevotella*. There is an overall growth of the whole microbial community, with *Pseudomonas* benefitting from the metabolic products from anaerobes. 4- The onset of clindamycin treatment suppresses the growth of gram-positive anaerobes, such as *Streptococcus* and *Staphylococcus*. The suppression of mucus-degrading bacteria removes the main nutritional source for *Pseudomonas*, leading to an overall decrease in microbial abundances. Period A corresponds to 28 days of hospitalization when the patient was treatment with colistin, vancomycin, piperacillin-tazobactam, and ceftazidime-avibactam; in period Period B the patient was released and was off antibiotics; Period C is the clindamycin treatment.

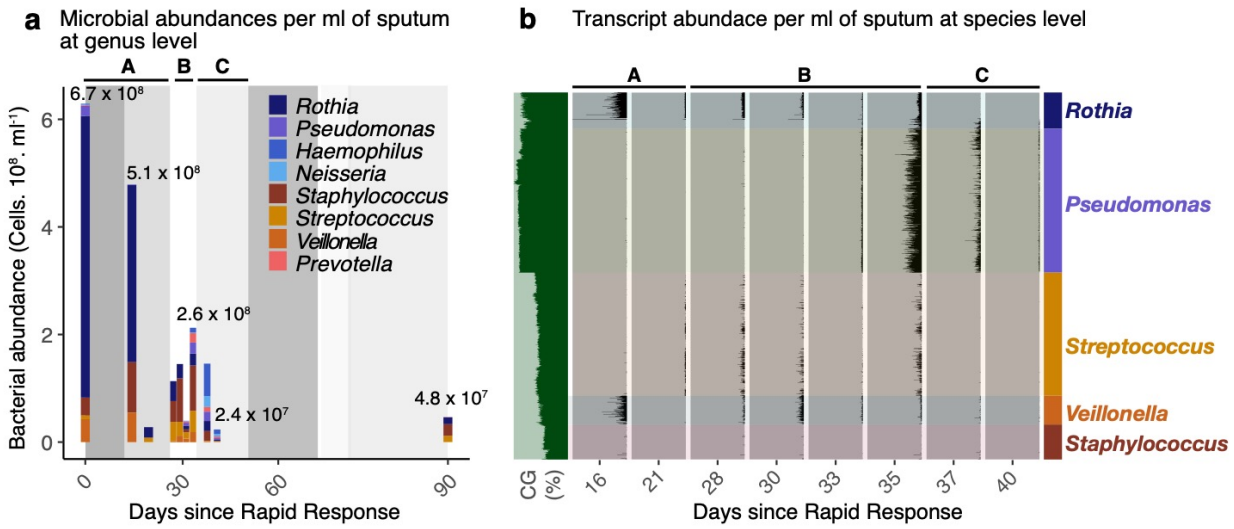

Figure 2. a) Changes in abundance of most abundant bacterial genera in the sputum from patient CF146. Absolute abundances (in cell counts per ml of sputum) were obtained by multiplying the fractional abundance from metagenomes by the total cell counts from epifluorescence microscopy. **b)** Recruitment of metatranscriptomic reads to contigs obtained from sequencing the genomes of clinical bacterial isolates. The height of each peak in the plot denotes mean coverage of a contig divided by overall sample mean coverage and scaled to the absolute microbial abundances per ml of sputum sample. As these are draft and not complete genomes, the position of each contig along the y axis is defined by k-mer similarity (k = 4) rather than position in the genome. The letters A, B and C within the plot area indicate the different antibiotic treatment periods.

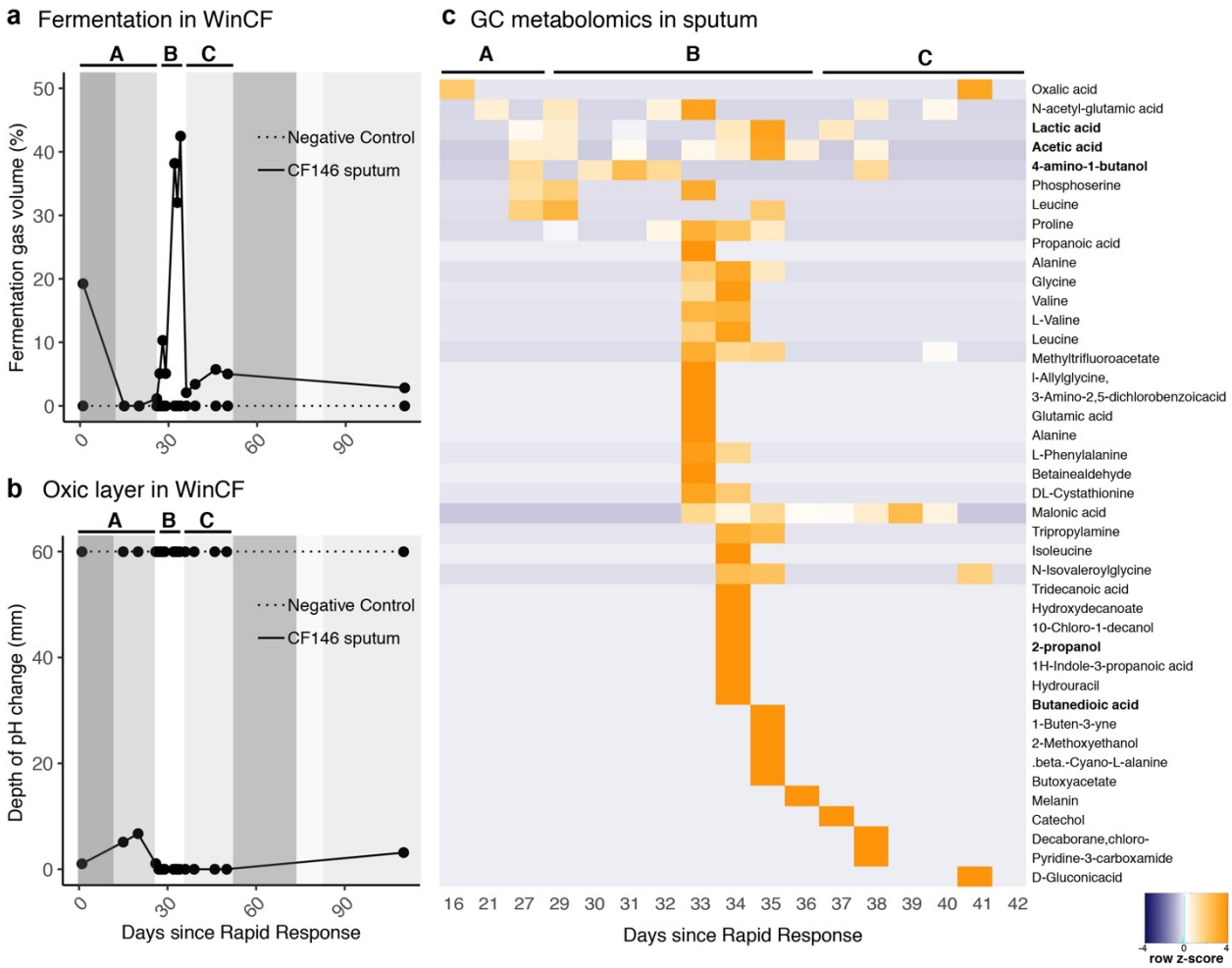

Figure 3. Fermentation in the sputum of patient CF146. **a**) production of fermentation gas in in WinCF capillary tubes inoculated with sputum microbial communities in artificial sputum media; **b**) depth of pH change in WinCF capillary tubes. The depth of tube where the pH changes corresponds to the transition from the oxic to anoxic environment and is analogous to the oxygen penetrance in the mucus plugs in the lung [29]. The letters A, B and C within the plot area indicate the different antibiotic treatment periods.

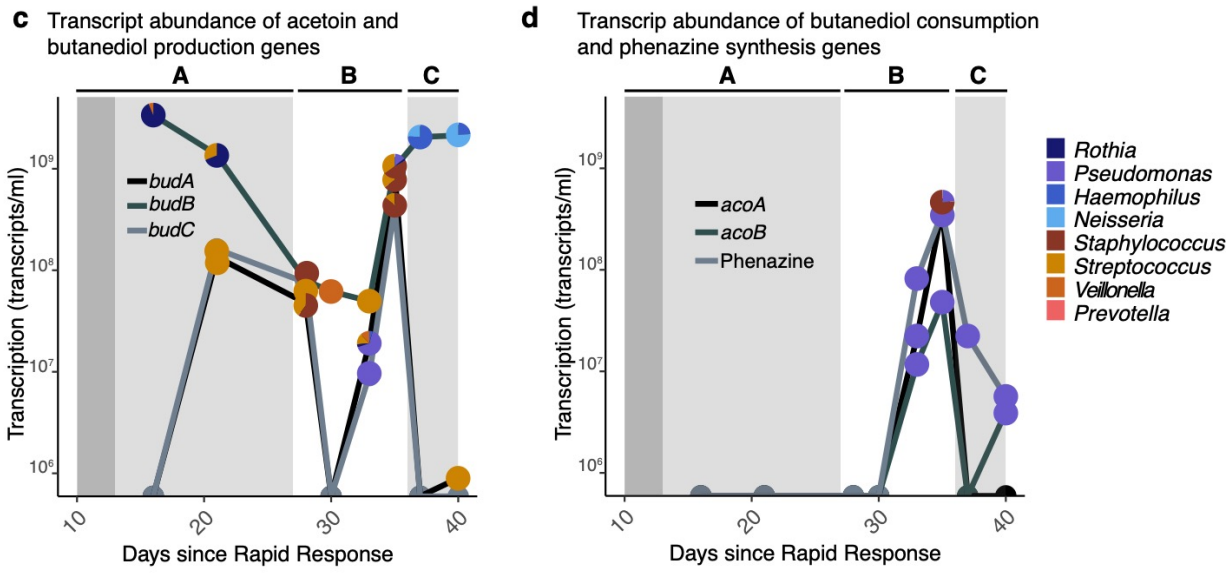

464

465

466 **Figure 4. Microbial transcriptome dynamics. a)** Abundance of transcripts involved in the

467 pathway of acetoin and butanediol production (*budA*, *budB*, and *budC*). Each point in the plot is

468 divided by the taxonomic assignment of the transcripts. The transcript abundance per ml (y axis)

469 was calculated as the product of the number of transcripts per Kb of a given taxon and the total

470 number of Kbs of a that same taxon, calculated from the absolute abundances and genome sizes.

471 **b)** Abundance of transcripts involved in the pathway of acetoin and butanediol consumption

472 (*acoA* and *acoB*) and phenazine production (*phzABCDEFG*, shown as a sum of all transcripts in

473 this gene cluster). Each point in the plot is divided by the taxonomic assignment of the

474 transcripts. The transcript abundance per ml (y axis) was calculated as in 4B.

475

476

477

478

Supplementary Figures

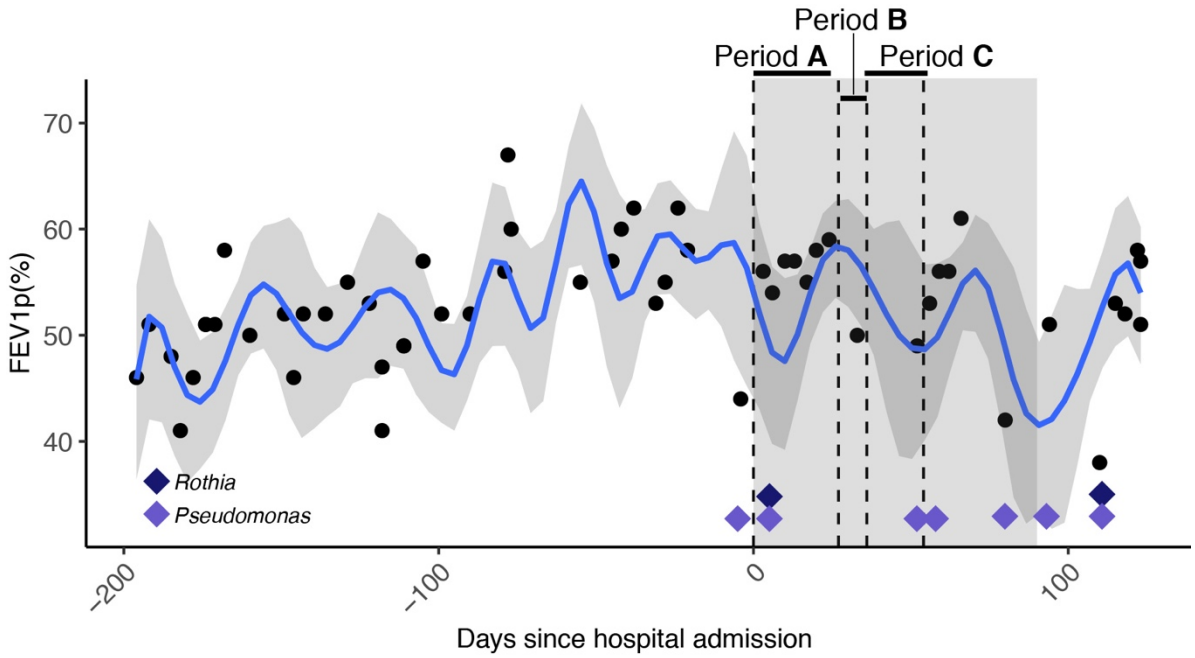

Figure S1. Patient's lung function over time. Day zero indicates the first day of hospitalization in the period focused on in this study. Percent predicted FEV1 (forced expiratory volume in one second) are shown by the dots; the blue line shows the median spline regression (effective degrees of freedom = 29). The shadow block indicates the window of time analyzed here by multi-omics. The diamond symbols indicate clinical microbiology tests positive for *Pseudomonas aeruginosa* and *Rothia* sp. during stand care. The vertical dotted lines indicate the three periods of interest in this study: Period A corresponds to 28 days of hospitalization when the patient was treatment with colistin, vancomycin, piperacillin-tazobactam, and ceftazidime-avibactam; in period Period B the patient was released and was off antibiotics; Period C is the clindamycin treatment.

References

1. Power ME, Tilman D, Estes JA, Menge BA, Bond WJ, Mills LS, et al. Challenges in the quest for keystones. Bioscience. 1996; September.

2. Cortés-Avizanda A, Colomer MÀ, Margalida A, Ceballos O, Donázar JA. Modeling the consequences of the demise and potential recovery of a keystone-species: wild rabbits and avian scavengers in Mediterranean landscapes. Sci Rep. 2015;2015 November:1–12. doi:10.1038/srep17033.

3. Pringle RM, Kartzinel TR, Palmer TM, Thurman TJ, Fox-dobbs K, Xu CCY, et al. Predator-induced collapse of niche structure and species coexistence. Nature. 2019. doi:10.1038/s41586-019-1264-6.

4. Hajishengallis G, Darveau RP, Curtis MA. The keystone-pathogen hypothesis. Nat Rev Microbiol. 2012;10:717–25. doi:10.1038/nrmicro2873.

5. Banerjee S, Schlaeppi K, Heijden MGA. functioning. Nat Rev Microbiol. 2018. doi:10.1038/s41579-018-0024-1.

6. Trosvik P, Jacques De Muinck E. Ecology of bacteria in the human gastrointestinal tract-identification of keystone and foundation taxa. 2015.

7. Röttjers L, Faust K. Can we predict keystones ? 2019;17 march:15007.

8. Roume H, Heintz-buschart A, Muller EEL, May P, Satagopam VP, Laczny CC, et al. Comparative integrated omics : identi fi cation of key functionalities in microbial community-wide metabolic networks. 2015; April.

9. Banerjee S, Schlaeppi K, Heijden MGA Van Der, Microbiol NR. Reply to ‘ Can we predict microbial keystones ?’ Nat Rev Microbiol. 2019;17 march:2019. doi:10.1038/s41579-018-0133-x.

10. Lawson CE, Harcombe WR, Hatzenpichler R. Common principles and best practices for engineering microbiomes. Nat Rev Microbiol. 2019.

11. Harris JK, De Groote MA, Sagel SD, Zemanick ET, Kapsner R, Penvari C, et al. Molecular identification of bacteria in bronchoalveolar lavage fluid from children with cystic fibrosis. Proc Natl Acad Sci. 2007;104:20529–33.

12. Quinton PM. Cystic fibrosis: impaired bicarbonate secretion and mucoviscidosis. Lancet. 2008;372:415–7.

13. Alaiwa MHA, Reznikov LR, Gansemer ND, Sheets KA, Horswill AR, Stoltz DA, et al. pH modulates the activity and synergism of the airway surface liquid antimicrobials β-defensin-3 and LL-37. Proc Natl Acad Sci. 2014;111:18703–8.

14. Kunzelmann K, Schreiber R, Hadorn HB. Bicarbonate in cystic fibrosis. J Cyst Fibros. 2017;16:653–62.

15. Gibson RL, Burns JL, Ramsey BW. Pathophysiology and management of pulmonary infections in cystic fibrosis. Am J Respir Crit Care Med. 2003;168:918–51.

16. Sibley CD, Parkins MD, Rabin HR, Duan K, Norgaard JC, Surette MG. A polymicrobial perspective of pulmonary infections exposes an enigmatic pathogen in Cystic Fibrosis patients. Proc Natl Acad Sci. 2008;105:15070–5.

17. Harrison F. Microbial ecology of the cystic fibrosis lung. Microbiology. 2007;153:917–23.

18. Tunney MM, Field TR, Moriarty TF, Patrick S, Doering G, Muhlebach MS, et al. Detection of anaerobic bacteria in high numbers in sputum from patients with cystic fibrosis. Am J Respir Crit Care Med. 2008;177:995–1001.

19. Lynch S V, Bruce KD. The cystic fibrosis airway microbiome. Cold Spring Harb Perspect Med. 2013;3:a009738.

539 20. Rogers GB, Carroll MP, Serisier DJ, Hockey PM, Jones G, Bruce KD. Characterization of
540 bacterial community diversity in cystic fibrosis lung infections by use of 16S ribosomal DNA
541 terminal restriction fragment length polymorphism profiling. J Clin Microbiol. 2004;42:5176–83.
542 21. Conrad D, Haynes M, Salamon P, Rainey PB, Youle M, Rohwer F. Cystic fibrosis therapy: a
543 community ecology perspective. Am J Respir Cell Mol Biol. 2013;48:150–6.
544 22. Whiteson KL, Bailey B, Bergkessel M, Conrad D, Delhaes L, Felts B, et al. The upper
545 respiratory tract as a microbial source for pulmonary infections in Cystic Fibrosis: parallels from
546 island biogeography. Am J Respir Crit Care Med. 2014;189:1309–15.
547 23. O'Toole GA. Cystic fibrosis airway microbiome: Overturning the old, opening the way for
548 the new. J Bacteriol. 2018;200:e00561-17.
549 24. Lim YW, Schmieder R, Haynes M, Willner D, Furlan M, Youle M, et al. Metagenomics and
550 metatranscriptomics: Windows on CF-associated viral and microbial communities. J Cyst Fibros.
551 2013;12:154–64. doi:10.1016/j.jcf.2012.07.009.
552 25. Lim YW, Evangelista JS, Schmieder R, Bailey B, Haynes M, Furlan M, et al. Clinical
553 insights from metagenomic analysis of sputum samples from patients with cystic fibrosis. J Clin
554 Microbiol. 2014;52:425–37.
555 26. Cowley ES, Kopf SH, LaRiviere A, Ziebis W, Newman DK. Pediatric cystic fibrosis sputum
556 can be chemically dynamic, anoxic, and extremely reduced due to hydrogen sulfide formation.
557 MBio. 2015;6:e00767-15.
558 27. Quinn RA, Lim W, Maughan H, Conrad D, Rohwer F, Whiteson L. Biogeochemical Forces
559 Shape the Composition and Physiology of Polymicrobial Communities in the Cystic Fibrosis
560 Lung. MBio. 2014;5:1–13.
561 28. Lim YW, Schmieder R, Haynes M, Furlan M, Matthews TD, Whiteson K, et al. Mechanistic

562 Model of *Rothia mucilaginosa* Adaptation toward Persistence in the CF Lung, Based on a
563 Genome Reconstructed from Metagenomic Data. PLoS One. 2013;8:e64285.
564 29. Quinn RA, Whiteson K, Lim Y-W, Salamon P, Bailey B, Mienardi S, et al. A Winogradsky-
565 based culture system shows an association between microbial fermentation and cystic fibrosis
566 exacerbation. ISME J. 2015;9:1024–38.
567 30. Whiteson KL, Meinardi S, Lim YW, Schmieder R, Maughan H, Quinn R, et al. Breath gas
568 metabolites and bacterial metagenomes from cystic fibrosis airways indicate active pH neutral 2,
569 3-butanedione fermentation. ISME J. 2014;8:1247.
570 31. Quinn RA, Whiteson K, Lim YW, Zhao J, Conrad D, LiPuma JJ, et al. Ecological
571 networking of cystic fibrosis lung infections. NPJ biofilms microbiomes. 2016;2:4.
572 32. Flynn JM, Niccum D, Dunitz JM, Hunter RC. Evidence and Role for Bacterial Mucin
573 Degradation in Cystic Fibrosis Airway Disease. 2016;:1–21.
574 33. Acosta N, Heirali A, Somayaji R, Surette MG, Workentine ML, Sibley CD, et al. Sputum
575 microbiota is predictive of long-term clinical outcomes in young adults with cystic fibrosis.
576 Thorax. 2018;73:1016–25.
577 34. Conrad DJ, Bailey BA, Hardie JA, Bakke PS, Eagan TML, Aarli BB. Median regression
578 spline modeling of longitudinal FEV1 measurements in cystic fibrosis (CF) and chronic
579 obstructive pulmonary disease (COPD) patients. PLoS One. 2017;12:e0190061.
580 35. Cobián Güemes AG, Lim YW, Quinn RA, Conrad DJ, Benler S, Maughan H, et al. Cystic
581 Fibrosis Rapid Response: Translating Multi-omics Data into Clinically Relevant Information.
582 MBio. 2019;10.
583 36. Phan J, Meinardi S, Barletta B, Blake DR, Whiteson K. Stable isotope profiles reveal active
584 production of VOCs from human-associated microbes. J Breath Res. 2017;11:17101.

585 37. Phan J, Gallagher T, Oliver A, England WE, Whiteson K. Fermentation products in the
586 cystic fibrosis airways induce aggregation and dormancy-associated expression profiles in a CF
587 clinical isolate of Pseudomonas aeruginosa. FEMS Microbiol Lett. 2018; March:1–11.
588 38. Gao B, Gallagher T, Zhang Y, Elbadawi-Sidhu M, Lai Z, Fiehn O, et al. Tracking
589 polymicrobial metabolism in cystic fibrosis airways: Pseudomonas aeruginosa metabolism and
590 physiology are influenced by Rothia mucilaginosa-derived metabolites. mSphere.
591 2018;3:e00151-18.
592 39. Root RK, Waldvogel F, Corey L, Stamm WE. Clinical infectious diseases: a practical
593 approach. Oxford University Press, USA; 1999.
594 40. Smith EE, Buckley DG, Wu Z, Saenphimmachak C, Hoffman LR, D'Argenio DA, et al.
595 Genetic adaptation by Pseudomonas aeruginosa to the airways of cystic fibrosis patients. Proc
596 Natl Acad Sci. 2006;103:8487–92.
597 41. Adamowicz EM, Flynn J, Hunter RC, Harcombe WR. Cross-feeding modulates antibiotic
598 tolerance in bacterial communities. ISME J. 2018;:2723–35. doi:10.1038/s41396-018-0212-z.
599 42. Climo MW, Israel DS, Wong ES, Williams D, Coudron P, Markowitz SM. Hospital-wide
600 restriction of clindamycin: effect on the incidence of Clostridium difficile-associated diarrhea
601 and cost. Ann Intern Med. 1998;128 12_Part_1:989–95.
602 43. Hankinson JL, Odencrantz JR, Fedan KB. Spirometric reference values from a sample of the
603 general US population. Am J Respir Crit Care Med. 1999;159:179–87.
604 44. Schluchter MD, Konstan MW, Drumm ML, Yankaskas JR, Knowles MR. Classifying
605 Severity of Cystic Fibrosis Lung Disease Using Longitudinal Pulmonary Function Data. Am J
606 Respir Crit Care Med. 2006;174:780–6. doi:10.1164/rccm.200512-1919OC.
607 45. Sriramulu DD, Lünsdorf H, Lam JS, Römling U. Microcolony formation: a novel biofilm

608 model of Pseudomonas aeruginosa for the cystic fibrosis lung. J Med Microbiol. 2005;54:667–
609 76.
610 46. Palmer KL, Aye LM, Whiteley M. Nutritional cues control Pseudomonas aeruginosa
611 multicellular behavior in cystic fibrosis sputum. J Bacteriol. 2007;189:8079–87.
612 47. Fung C, Naughton S, Turnbull L, Tingpej P, Rose B, Arthur J, et al. Gene expression of
613 Pseudomonas aeruginosa in a mucin-containing synthetic growth medium mimicking cystic
614 fibrosis lung sputum. J Med Microbiol. 2010.
615 48. Cantu VA, Sadural J, Edwards R. PRINSEQ++, a multi-threaded tool for fast and efficient
616 quality control and preprocessing of sequencing datasets. PeerJ Prepr. 2019;7:e27553v1.
617 49. Ponstingl H, Ning Z. SMALT-a new mapper for DNA sequencing reads. F1000 Posters.
618 2010;1:313.
619 50. Bankevich A, Nurk S, Antipov D, Gurevich AA, Dvorkin M, Kulikov AS, et al. SPAdes: a
620 new genome assembly algorithm and its applications to single-cell sequencing. J Comput Biol.
621 2012;19:455–77.
622 51. Smart KF, Aggio RBM, Van Houtte JR, Villas-Bôas SG. Analytical platform for
623 metabolome analysis of microbial cells using methyl chloroformate derivatization followed by
624 gas chromatography–mass spectrometry. Nat Protoc. 2010;5:1709.
625 52. Eren AM, Esen ÖC, Quince C, Vineis JH, Morrison HG, Sogin ML, et al. Anvi'o: an
626 advanced analysis and visualization platform for 'omics data. PeerJ. 2015;3:e1319.
627 53. Cobián Güemes AG, Youle M, Cantú VA, Felts B, Nulton J, Rohwer F. Viruses as winners
628 in the game of life. Annu Rev Virol. 2016;3:197–214.
629 54. Li H. Microbiome, metagenomics, and high-dimensional compositional data analysis. Annu
630 Rev Stat Its Appl. 2015;2:73–94.

631 55. Thompson J, Johansen R, Dunbar J, Munsky B. Machine learning to predict microbial
632 community functions: An analysis of dissolved organic carbon from litter decomposition.
633 BioRxiv. 2019;:599704.
634

Figures

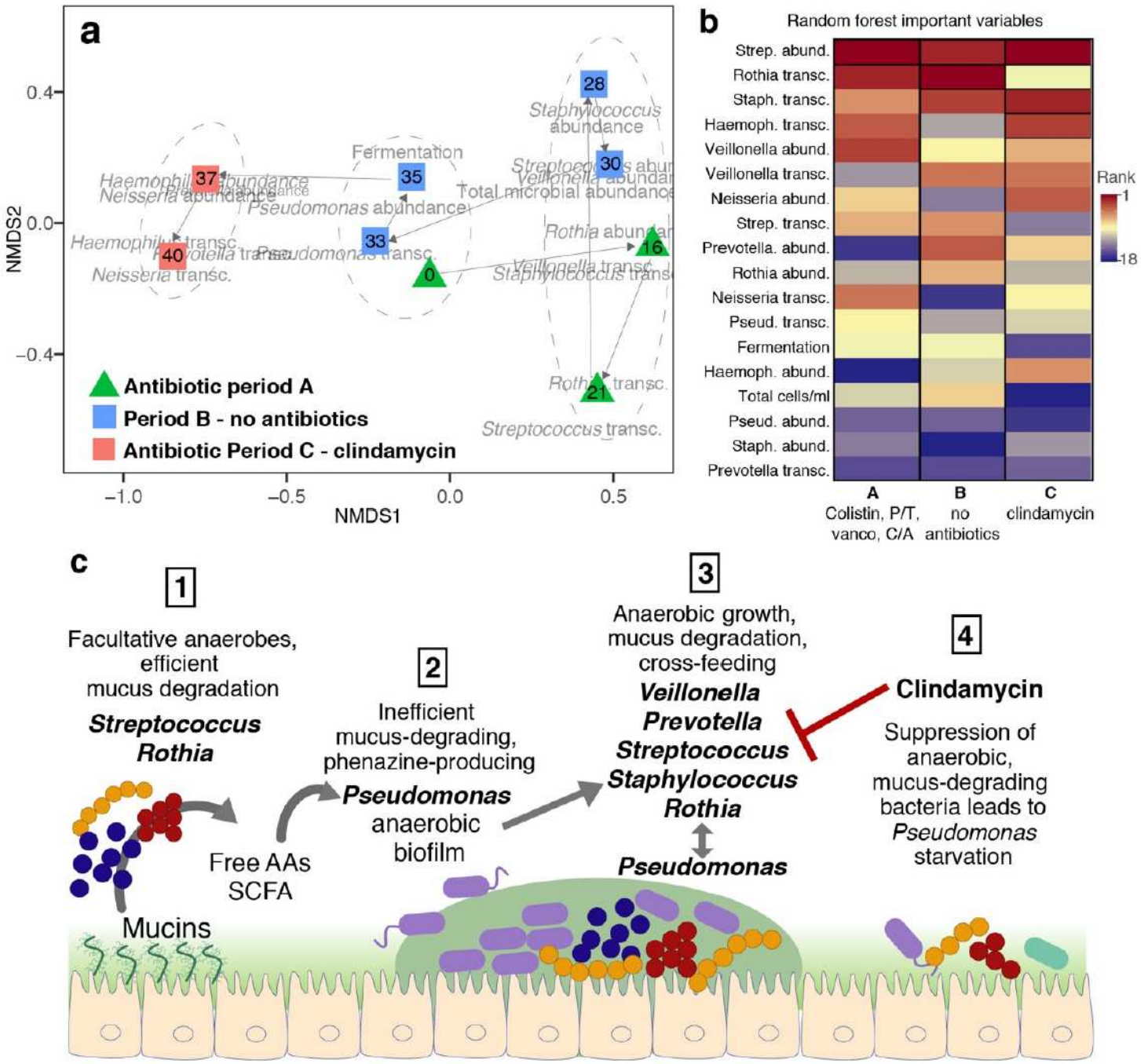

Figure 1

Microbial community succession. a) Non-metric multidimensional scaling (NMDS) of sputum samples over time. The variables used as input for the NMDS were WinCF fermentation, total microbial abundances, genera-specific microbial abundances, and genera specific transcriptomic activity. Symbols are color-coded by antibiotic treatment periods (green: A - colistin, vancomycin, ceftazidime-avibactam, and piperacillin-tazobactam; blue: B - no antibiotics; pink: C - clindamycin), and numbers inside the

symbols indicate days since hospital admission event when Rapid Response was initiated. The dotted ellipses indicate health status groups supported by an unsupervised random forest analysis followed by clustering using Ward distances (out of bag error = 11.1 %). b) Important variables differentiating treatment periods in a classification random forest analysis supervised by treatments. The ranks surrounded by a black box indicate variables with p-values less than 0.05 in the permutational test. c) Conceptual model of succession events in patient CF146: 1- The mucosal surfaces are colonized by facultative anaerobes, including Streptococcus and Rothia, capable of efficient mucus degradation producing free-amino acids and short-chain fatty acids (SCFA, i.e., propionate, acetate, butyrate, and butanediol). 2- The free amino acids and SCFAs open a niche for the growth of Pseudomonas, which degrades mucins poorly. Pseudomonas grows forming an anaerobic biofilm, and produces phenazines. 3- The Pseudomonas biofilm facilitates the growth of anaerobes, including obligate anaerobes such as Veillonella and Prevotella. There is an overall growth of the whole microbial community, with Pseudomonas benefitting from the metabolic products from anaerobes. 4- The onset of clindamycin treatment suppresses the growth of gram positive anaerobes, such as Streptococcus and Staphylococcus. The suppression of mucus degrading bacteria removes the main nutritional source for Pseudomonas, leading to an overall decrease in microbial abundances. Period A corresponds to 28 days of hospitalization when the patient was treatment with colistin, vancomycin, piperacillin-tazobactam, and ceftazidime avibactam; in period Period B the patient was released and was off antibiotics; Period C is the clindamycin treatment.

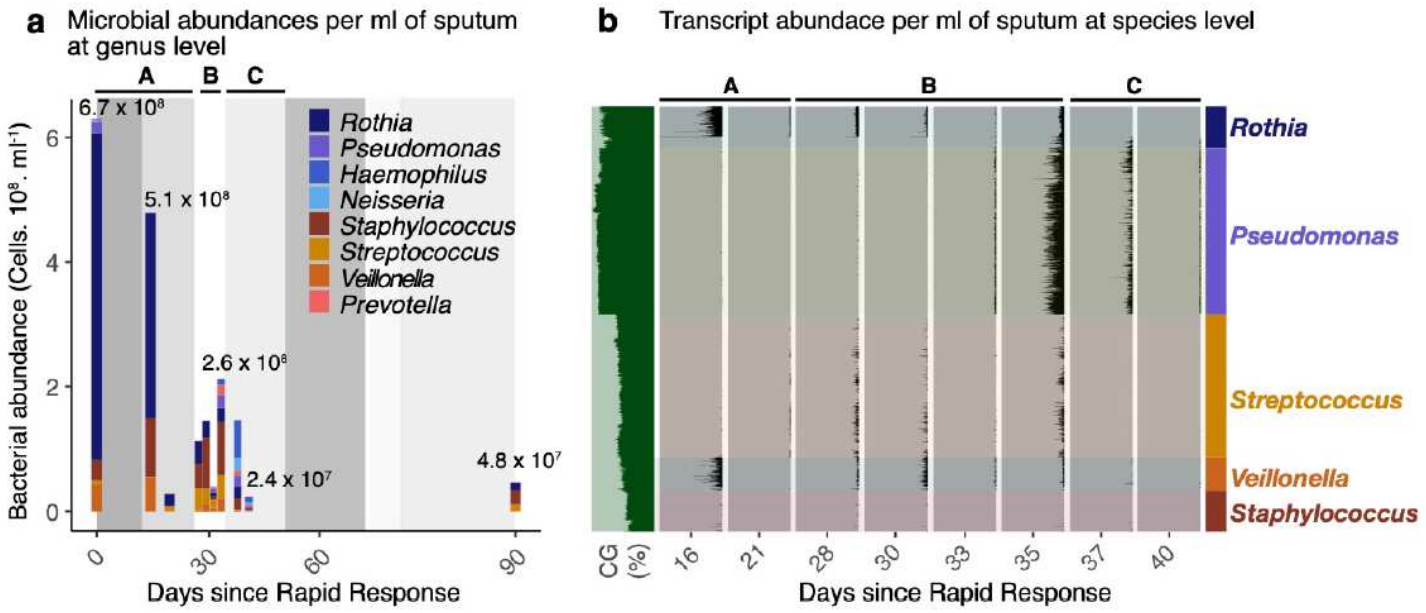

Figure 2

a) Changes in abundance of most abundant bacterial genera in the sputum from patient CF146. Absolute abundances (in cell counts per ml of sputum) were obtained by multiplying the fractional abundance from metagenomes by the total cell counts from epifluorescence microscopy. b) Recruitment of metatranscriptomic reads to contigs obtained from sequencing the genomes of clinical bacterial isolates.

The height of each peak in the plot denotes mean coverage of a contig divided by overall sample mean coverage and scaled to the absolute microbial abundances per ml of sputum sample. As these are draft and not complete genomes, the position of each contig along the y axis is defined by k-mer similarity (k = 4) rather than position in the genome. The letters A, B and C within the plot area indicate the different antibiotic treatment periods.

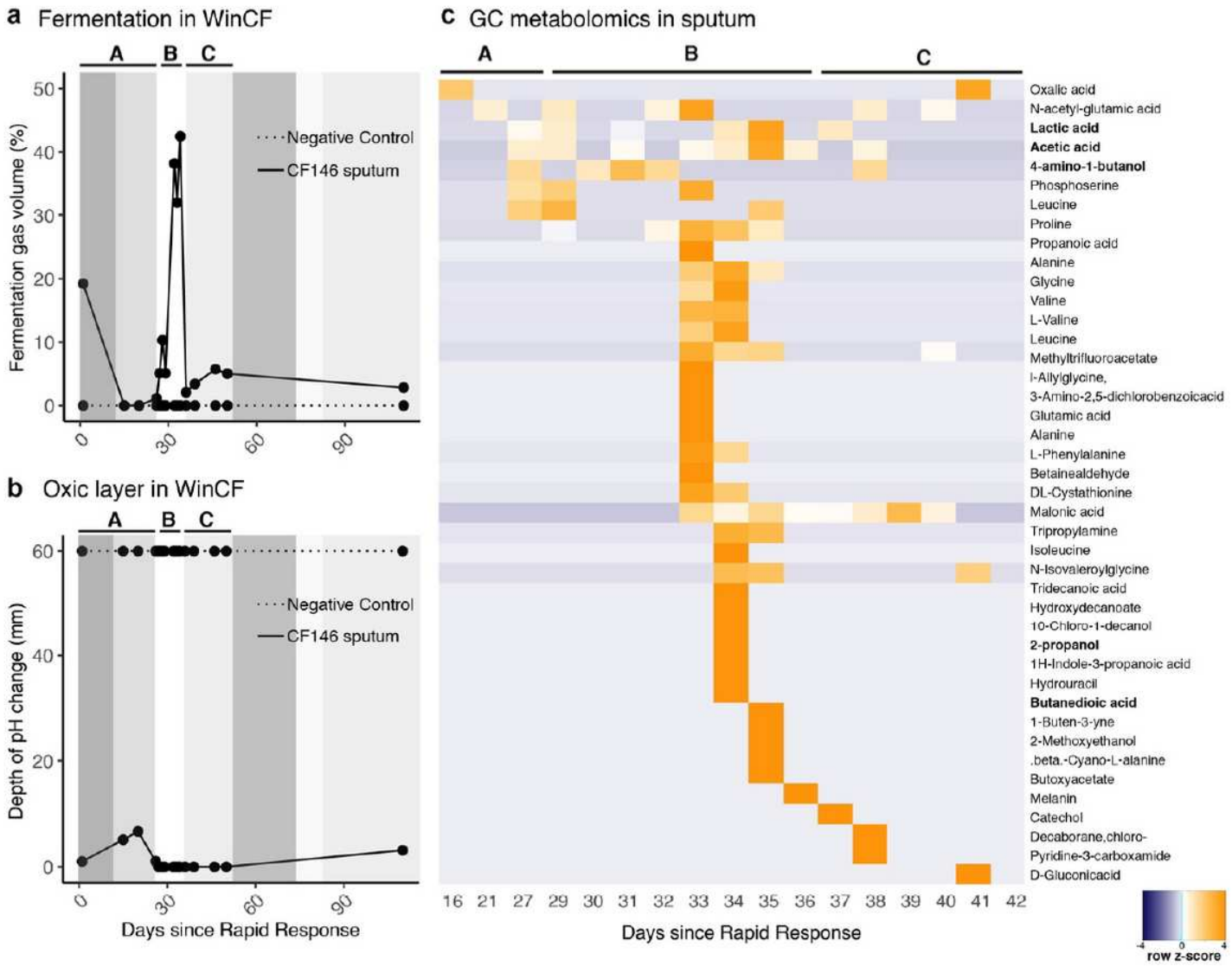

Figure 3

Fermentation in the sputum of patient CF146. a) production of fermentation gas in in WinCF capillary tubes inoculated with sputum microbial communities in artificial sputum media; b) depth of pH change in WinCF capillary tubes. The depth of tube where the pH changes corresponds to the transition from the oxic to anoxic environment and is analogous to the oxygen penetrance in the mucus plugs in the lung [29]. The letters A, B and C within the plot area indicate the different antibiotic treatment periods.

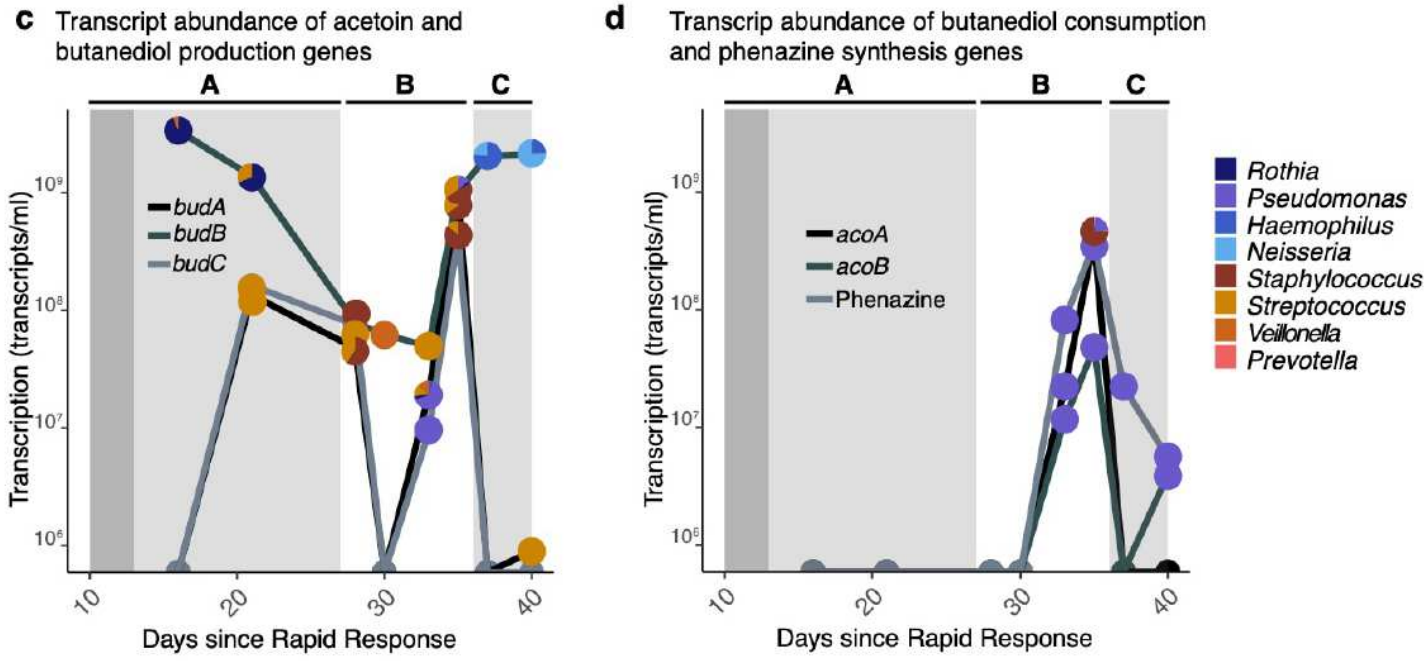

Figure 4

Microbial transcriptome dynamics. c) Abundance of transcripts involved in the pathway of acetoin and butanediol production (budA, budB, and budC). Each point in the plot is divided by the taxonomic assignment of the transcripts. The transcript abundance per ml (y axis) was calculated as the product of the number of transcripts per Kb of a given taxon and the total number of Kbs of a that same taxon, calculated from the absolute abundances and genome sizes. d) Abundance of transcripts involved in the pathway of acetoin and butanediol consumption (acoA and acoB) and phenazine production (phzABCDEFG, shown as a sum of all transcripts in this gene cluster). Each point in the plot is divided by the taxonomic assignment of the transcripts. The transcript abundance per ml (y axis) was calculated as in 4d.

Supplementary Files

This is a list of supplementary files associated with this preprint. Click to download.

- CF146alldataforstats.csv
- CF146Rscriptsforpublication.R
- CF146fev.csv